Journal of The Electrochemical Society, **152** (9) G698-G702 (2005)
0013-4651/2005/152(9)/G698/5/$7.00 © The Electrochemical Society, Inc.

Synthesis and the Luminescent Properties of Ba_2ZnS_3:Ce,Ag Phosphors

Yu-Feng Lin, Yen-Hwei Chang,[z] and Bin-Siang Tsai

Department of Materials Science and Engineering, National Cheng Kung University, Tainan, 701 Taiwan

Ba_2ZnS_3:Ce,Ag phosphors, emitting bluish to yellowish-green light, were synthesized by a double-crucible method. X-ray diffraction results indicate that the raw materials were completely sulfurized at 1000°C for 2 h, and all samples had a orthorhombic crystal structure with doping 0.1-1 mol % Ce^{3+} and codoping 0-0.2 mol % Ag^+. The emission spectra resulted from (*i*) host-activator transition and (*ii*) $^2D(5d)$-$^7F_{5/2}(4f)$ and $^2D(5d)$-$^7F_{7/2}(4f)Ce^{3+}$ transitions. The photoluminescence spectra show that the emission peaks in the 494-508 nm range (excited at λ_{exc} = 420 nm) and in the 493-537 nm range (excited around λ_{exc} = 356 nm), like the CIE color coordinate, depend on the doping concentration of the Ce^{3+} and Ag^+ ions.
 [DOI: 10.1149/1.1954947]

Manuscript submitted January 25, 2005; revised manuscript received March 21, 2005. Available electronically July 21, 2005.

II-VI compounds with wide bandgaps, such as zinc chalcogenide ZnS and alkaline-earth chalcogenides (AES) MgS,[1,2] CaS,[3,4] SrS,[5,6] and BaS[7] are promising for optoelectronic applications. Rare-earth metals are known to be efficient luminescent materials for the realization of multicolor electroluminescent and cathodoluminescent devices.[8] Interest in Ce-doped wide-bandgap phosphor materials with full color luminescence is considerable because such materials have the potential to generate blue light with broad-band emission from the 5d-4f transition of Ce^{3+}. The Ce^{3+} ion is known to have the [Xe] $4f^1$ configuration, which results in only two $4f^1$ energy levels, the $^2F_{5/2}$ ground state and the $^2F_{7/2}$ excited state. These energy levels are approximately 2000 cm^{-1} apart.[9] The $4f^05d^1$ bands can be found at higher energy. The 5d level of the Ce^{3+} depends strongly on the crystal field of the host crystal. The peak position of Ce^{3+} emission shifts according to the host material.[8] Hence, several II-VI mixed sulfides doped with rare-earth ions have been investigated, $Ca_{1-x}Sr_xS$:Ce,[10] $Ca_{1-x}Sr_xS$:Eu,[11] and $Zn_{1-x}Sr_xS$:Ce.[12]

Barium zinc sulfide was first prepared by Hoppe[13] by firing zinc oxide and barium oxide in an atmosphere of hydrogen sulfide (H_2S). Subsequently, Megson investigated the solubility of ZnS in BaS.[14] The firing of BaS and ZnS (in the molar ratio 2BaS:1ZnS) in an oxygen-free nitrogen atmosphere yielded barium zinc sulfide (Ba_2ZnS_3). However, the roles of the rare earth ion Ce^{3+} and the transition metal ion Ag^+ codoped in barium zinc sulfide have not yet been studied.

In this investigation, the Ce^{3+} and Ag^+ codoped barium zinc sulfide phosphors were synthesized using the double-crucible method to control the doping concentration of Ce^{3+} and Ag^+ ions in a conventional solid-state reaction. The phases, morphologies, and photoluminescent properties of Ba_2ZnS_3:Ce^{3+}, Ag^+ phosphors were studied.

Experimental

Sample preparation.— Ba_2ZnS_3:Ce^{3+}, Ag^+ phosphors were synthesized in two steps in this experimental procedure. Pure barium sulfide was produced first using starting ingredients of $BaCO_3$ (Noah), S (Showa), and ethanol (ACS reagent, Acros). Two crucibles were put into a quartz tube furnace,[15] one containing the well-mixed $BaCO_3$ and S and the other containing the proper amount of ethanol as a reducing agent. The contents were fired at 1000°C for 2 h.

In the second step, samples of Ba_2ZnS_3:*x*Ce, *y*Ag, with $0.1 \leqq x \leqq 1.0$ and $0 \leqq y \leqq 0.2$ mol %, were prepared via the conventional solid-state reaction using the double-crucible method. The starting ingredients consisted of BaS, ZnS (Cerac), S (Showa), $CeCl_3 \cdot 7H_2O$ (Alfa), $AgNO_3$ (Riedel-de Haën), and ethanol. The required amounts of $CeCl_3 \cdot 7H_2O$ and $AgNO_3$ were first dissolved in an aqueous ethanol. The stoichiometric amounts of BaS, ZnS, and S were added to the ethanol solution and mixed during continuous stirring for 1 h at about 65°C until all ethanol was evaporated. Subsequently, the aforementioned two-crucibles method was used again. These two crucibles were put into a quartz-tube furnace and fired at 1000°C for 2 h. Ethanol is also a reducing agent and produces a reductive atmosphere.

Characterization.— The effects of Ce, Ag doping, and of thermal treatment on the structure were carefully studied by X-ray powder diffraction (XRD) using Cu Kα radiation (Rigaku Dmax-33 X-ray diffractometer) with a source power of 30 kV and a current of 20 mA. The surface morphology was examined by high-resolution scanning electron microscopy (HR-SEM, S4200, Hitachi). Both excitation and luminescence spectra of these phosphors were recorded on a Hitachi F-4500 fluorescence spectrophotometer using a 150 W xenon arc lamp as the excitation source at room temperature.

Results and Discussion

Structures.— All the peaks in the X-ray powder diffraction patterns of Ba_2ZnS_3:*x*Ce with $0 \leqq x \leqq 1.0$ mol % were identified to correspond to the orthorhombic Ba_2ZnS_3 phase with space group *Pnam* (no. 62). The X-ray patterns present a pure Ba_2ZnS_3 phase (as shown in Fig. 1) as well as Ce doping, and codoping with Ag^+ to 0.2 mol %.

Figure 2 plots the dependence of the full width at half-maximum (fwhm) of the (131) peaks on Ce^{3+} concentration. The fwhm of Ba_2ZnS_3:Ce^{3+} increased with the doping Ce^{3+} concentration. The trivalent cerium ion was introduced at a divalent cation site; defects were generated and the crystallinity was poor. As small concentrations of Ce^{3+} ions ($\leqslant$0.3 mol %) and Ag^+ ions (0.1 mol %) were codoped, the crystallinity of the samples increased. However, when the doping concentration of Ce^{3+} ions exceeded 0.3 mol % or the codoping concentration of Ag^+ ions was 0.2 mol %, the fwhm values became large and the crystallinity decreased. The crystallility was highest when the sample was doped with 0.2 mol % Ce^{3+} and 0.1 mol % Ag^+ ions. Regardless of codoped Ag^+ ions, the crystallinity of Ba_2ZnS_3:Ce^{3+} powders depended strongly on the concentration of Ce^{3+} ions. Furthermore, the fwhm of the pure Ba_2ZnS_3 sample was 0.231°, so the pure crystal was less crystalline than the slightly doped crystals.

The morphology of the Ba_2ZnS_3 powders doped with 0.1-1.0 mol % Ce^{3+} ions does not differ markedly from that of the powders codoped with 0.1-0.2 mol % Ag^+ ions. The SEM images show that those particles are irregularly shaped with sizes of between 3 and 10 μm. Some small particles are sintered to form a large one, possibly because the temperature is high and the soaking is long.

Optical properties.— Trivalent Ce^{3+} ions have an electronic structure with one 4f electron, and when used as an activator, they generally result in phosphors with broad band emission. The mea-

[z] E-mail: enphei@mail.ncku.edu.tw

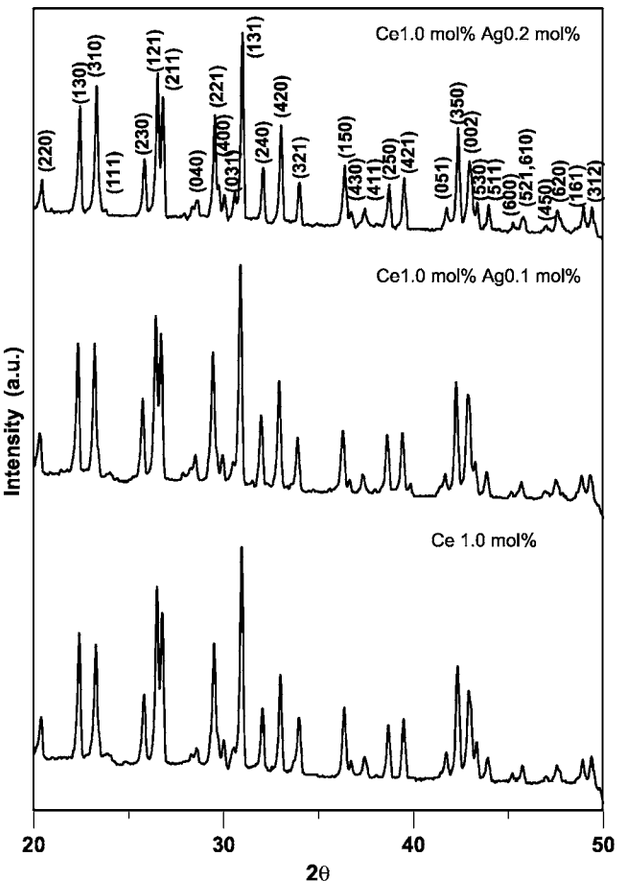

Figure 1. XRD patterns of Ba_2ZnS_3-doped Ce^{3+} 1.0 mol % and codoped Ag^+ 0.1, 0.2 mol % ions.

sured excitation spectra of the Ba_2ZnS_3:Ce phosphors reveal two excited bands with peaks at around 360 and 420 nm. Figure 3 presents emission spectra excited by light at around 360 nm.

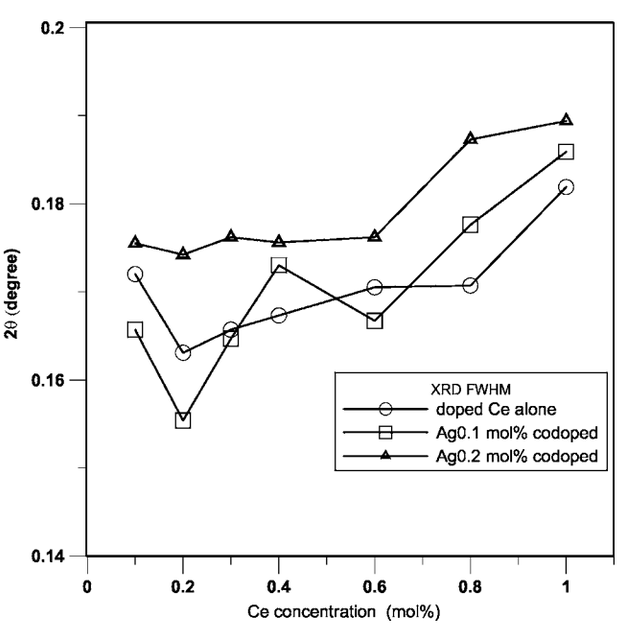

Figure 2. The relationship of fwhm of (131) peak and Ce^{3+} concentration of Ba_2ZnS_3:Ce^{3+}, Ag^+ phosphors.

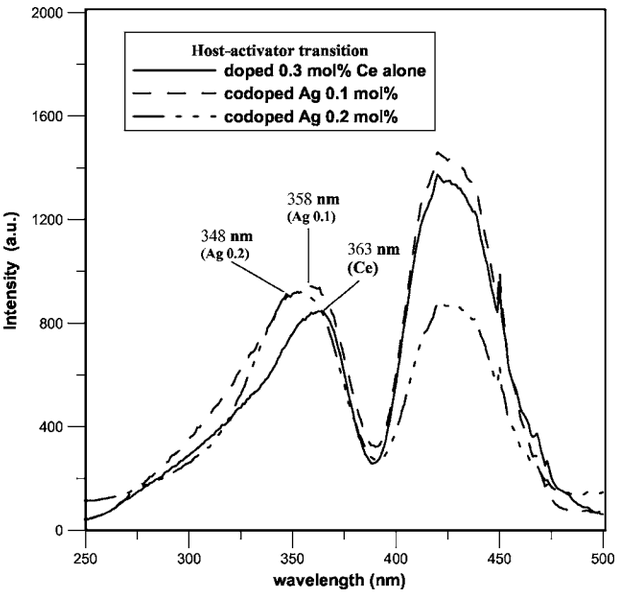

Figure 3. Emission spectra of Ba_2ZnS_3 doping with 0.3 mol % Ce^{3+} ions alone and codoped with 0.1 and 0.2 mol % Ag^+ ions were measured under the excited wavelength at 363, 358, and 348 nm, respectively.

Host-activator transition.— The first broad band of the photoluminescent (PL) excitation spectrum ranges from 250 to 390 nm because of the energy transition between the host and the activator.[15] The peaks of the first excitation band at around 360 nm (~3.5 eV) coincide with the bandgap of the semiconductor Ba_2ZnS_3, suggesting that part of the total energy of the emitted light comes from the energy absorbed by the host. Figure 4 presents the PL excitation spectra of Ba_2ZnS_3 doped with 0.3 mol % Ce^{3+} ions

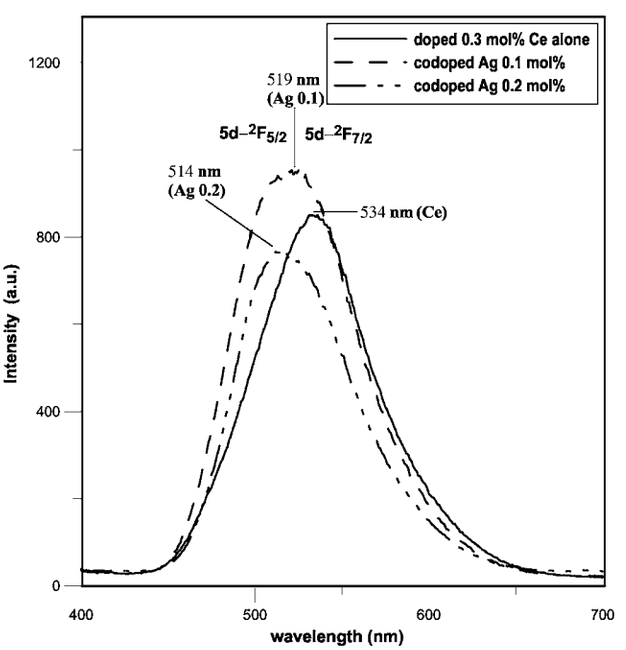

Figure 4. Excitation spectra of Ba_2ZnS_3 doping with 0.3 mol % Ce^{3+} ions alone and codoped with 0.1 and 0.2 mol % Ag^+ ions were measured from the emission peaks at around 514-534 nm.

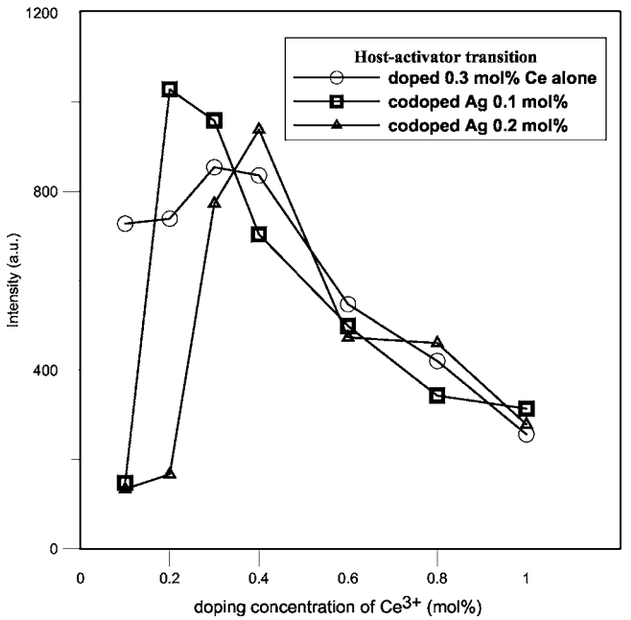

Figure 5. The relationship of PL intensity and Ce^{3+} concentration excited at $\lambda_{exc} \approx 358$ nm.

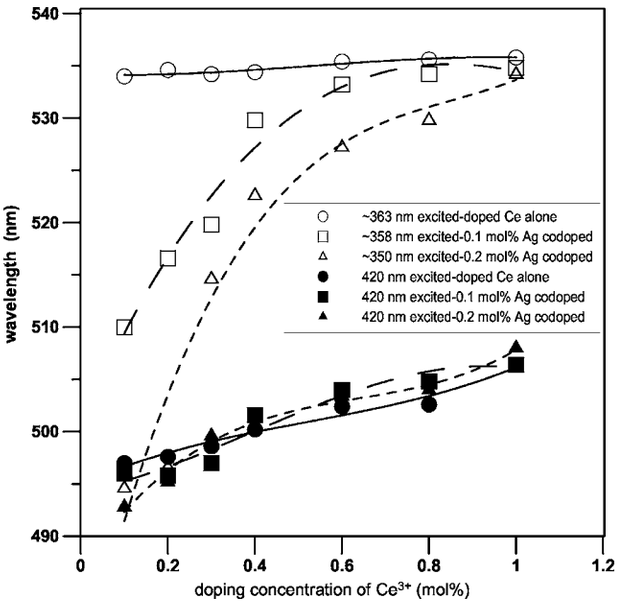

Figure 6. The relationship of wavelengths of emission peak of $Ba_2ZnS_3:Ce^{3+}$, Ag^+ phosphors and Ce^{3+} concentration, excited at $\lambda_{exc} \approx 358$ nm and $\lambda_{exc} = 420$ nm.

and codoped with 0.1 and 0.2 mol % Ag^+ ions, measured at the emission peaks at around 514-534 nm. The peaks of the first broad excited bands at 363, 358, and 348 nm correspond to the samples doped with 0.3 mol % Ce^{3+}, 0.1 mol % Ag^+, and 0.2 mol % Ag^+, respectively. Doping with more Ag^+ ions corresponds to a lower wavelength of the excitation peak.

The PL emission spectra of $Ba_2ZnS_3:Ce^{3+}$ and $Ba_2ZnS_3:Ce^{3+}$, Ag^+ phosphors have a broad emission band between 440 and 660 nm because of 5d-4f Ce^{3+} luminescence. When the wavelength is transformed to energy, the $^2F_{5/2}$ and $^2F_{7/2}$ levels are fitted by two Gaussian-shaped peaks at around 20,410 cm^{-1} (2.53 eV) and 18,350 cm^{-1} (2.28 eV) below the lowest 5d excited state. The spin-orbital splitting of the ^2F ground state is about 2060 cm^{-1}, which is typical for Ce^{3+}.[16] The blue shift was observed as the concentrations of Ag^+ ions increased as the proportions of these two transitions differed (5d-$^2F_{5/2}$ and 5d-$^2F_{7/2}$). The emission peak at 534 nm for Ba_2ZnS_3 doped with 0.3 mol % Ce^{3+} ions was shifted to 519 and 514 nm by codoping with 0.1 and 0.2 mol % Ag^+, respectively. The luminescent intensity of these phosphor materials depends strongly on the activator concentration, as shown in Fig. 5. When the doping concentration of Ce^{3+} ions was 0.3 mol %, the maximum emission intensity was obtained. The phenomenon of concentration quenching occurred as the doping concentration of Ce^{3+} ions was above 0.3 mol %. Codoping with 0.1 mol % Ag^+ increased the PL intensity. Figure 6 presents the relationship between the wavelengths of the emission peaks and the activator doping concentration. Doping with 0.1-1.0 mol % Ce^{3+} alone slightly red-shifted the emission peaks (excited at about 363 nm) from 534 to 536 nm. The $Ba_2ZnS_3:Ce^{3+}$ phosphors codoped with Ag^+ ions exhibit a red-shift that increases with the concentration of Ce^{3+} ions. Codoping with 0.1 mol % Ag^+ ions shifts the emission peak from 510 to 535 nm as the Ce^{3+} ion content increases from 0.1 to 1.0 mol %. 0.2 mol % Ag^+ codoped samples also exhibited this phenomenon, with a red-shift from 495 to 534 nm for the same range of Ce^{3+} ions. Therefore, the sample codoped with 0.2 mol % Ce^{3+} and 0.1 mol % Ag^+ exhibited the highest PL intensity at $\lambda_{em} = 516$ nm when excited by 360 nm UV rays.

Activator direct transition.— The second broad band of the PL excitation spectrum ranges between 390 and 475 nm because of the 4f-5d energy transition of Ce^{3+} ions. The crystal field interaction influences the positions of the $4f^05d^1$ levels much more strongly than the positions of the $4f^1$ levels because of a strong interaction of the 5d-electron with the neighboring anion ligands in the compound. Figure 7 shows the excitation spectra of the samples doped with 0.3 mol % Ce^{3+} ions and of those codoped with 0.1 and 0.2 mol % Ag^+ ions. The spectra were measured from the emission peak at around 500 nm. The same wavelength of the peaks of the second broad excited band at 420 nm was observed. Several salient peaks at 420, 438, 450, 468, and 473 nm on the second broad excited band were caused by the crystal field effect.

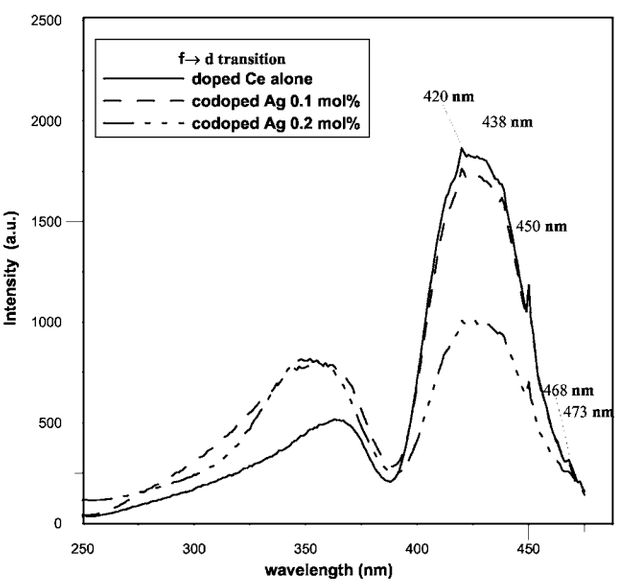

Figure 7. Excitation spectra of Ba_2ZnS_3 doped with 0.3 mol % Ce^{3+} ions alone and codoped with 0.1 and 0.2 mol % Ag^+ ions were measured from the emission peaks at around 500 nm.

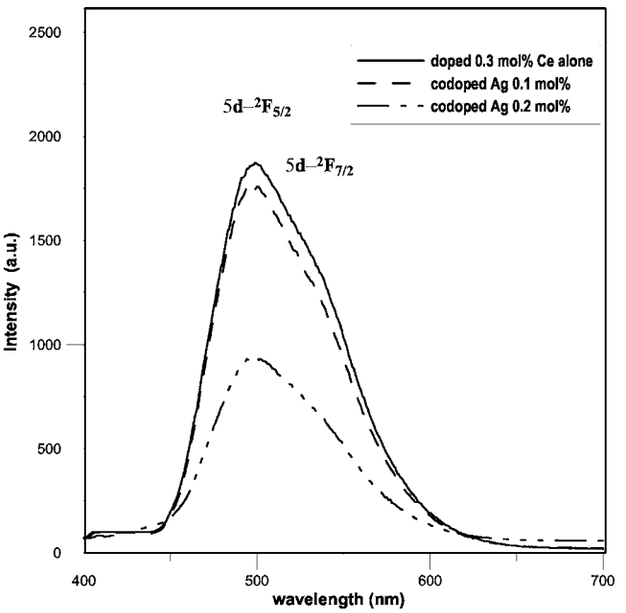

Figure 8. Emission spectra of Ba_2ZnS_3 doped with 0.3 mol % Ce^{3+} ions alone and codoped with 0.1 and 0.2 mol % Ag^+ ions were measured under the excited wavelength at 420 nm.

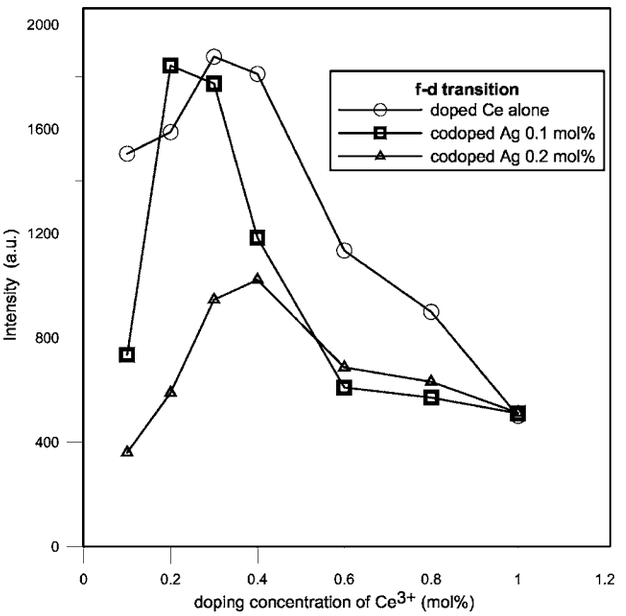

Figure 9. The relationship of PL intensity of Ba_2ZnS_3:Ce^{3+}, Ag^+ phosphors and doped Ce^{3+} concentration excited at λ_{exc} = 420 nm.

Under the 422 nm blue ray excitation, the energy absorbed directly by the Ce^{3+} ion corresponded to the transition from the 4f ground state to the 5d excited state. As the doping concentration of Ce^{3+} ions increased from 0.1 to 1.0 mol %, the emission peaks were red-shifted from 496 to 508 nm, as shown in Fig. 6. The wavelengths of the emission peaks do not obviously differ, in spite of the amount of doping or codoping. However, the redshift depends more strongly on the concentration of the Ce^{3+} ions than on the concentration of the codoped Ag^+ ions. In Fig. 8, the wavelengths of the emission peaks of Ba_2ZnS_3 doped with 0.3 mol % Ce^{3+} ions alone and codoped with Ag^+ ions 0.1 and 0.2 mol % were around 500 nm with a shoulder peak at about 545 nm, corresponding to 5d-$^2F_{5/2}$ and 5d-$^2F_{7/2}$ transitions, respectively. The luminescence intensity decreases as the concentration of codoped Ag^+ ions increases. At a given Ce^{3+} doping level, the luminescence intensities of the codoped Ag^+ samples were all lower than those of the uncodoped samples, except for the sample codoped with 0.2 mol % Ce^{3+} and 0.1 mol % Ag^+ ions, which yielded the highest intensity, as shown in Fig. 9.

Figure 10 displays the CIE color coordinates of all samples excited by an ~358 nm UV-ray and 420 nm blue light. Excited by a ~358 nm UV-ray, the emission peak of the phosphors exhibited a large redshift and the CIE color coordinates were widely distributed over bluish-green, green, and yellowish-green regions. The CIE color coordinates of the sample doped only with Ce^{3+} were all in the yellowish-green region (from $x = 0.2817$, $y = 0.5653$ to $x = 0.3061$, $y = 0.5832$); those of the Ba_2ZnS_3:Ce^{3+} phosphors codoped 0.1 mol % Ag^+ were in the green ($x = 0.2147$, $y = 0.4916$) to yellowish-green ($x = 0.3002$, $y = 0.5856$) region; and those of the phosphors codoped with 0.2 mol % Ag^+ were in the bluish-green ($x = 0.1772$, $y = 0.3999$) to yellowish-green ($x = 0.3030$, $y = 0.5863$) region.

Excited by 420 nm blue light, the samples emitted green light and the CIE color coordinates were spread between $x = 0.1818$, $y = 0.4212$ and $x = 0.2289$, $y = 0.5244$. Redshift increased with Ce^{3+} ion doping.

Conclusion

Ce^{3+}-doped and Ag^+ codoped Ba_2ZnS_3 phosphor powders were successfully synthesized via a conventional solid-state reaction using a double-crucible method. Ba_2ZnS_3:*x*Ce, *y*Ag powders calcined at 1000°C for 2 h have a single orthorhombic structure and exhibited efficient emission following excitement by a UV-ray with $\lambda_{exc} \approx 358$ and 420 nm. A comparison with the phosphors doped with Ce^{3+} alone revealed that the emission peak of Ag^+ codoped samples was markedly blueshifted when the samples were excited by UV-rays with $\lambda_{exc} \approx 358$ nm. The sample doped with 0.2 mol % Ce^{3+} and 0.1 mol % Ag^+ ions has a maximum PL intensity and yellowish-green light emission at 516 nm with a CIE color coordinate of $x = 0.347$, $y = 0.538$. The emission peaks of the Ba_2ZnS_3:*x*Ce, *y*Ag phosphors were more redshifted as the concentration of the Ce^{3+} ions increased when the samples were excited by $\lambda_{exc} \approx 358$ or 420 nm. Excitation at λ_{exc} = 420 nm caused the sample of Ba_2ZnS_3:0.3

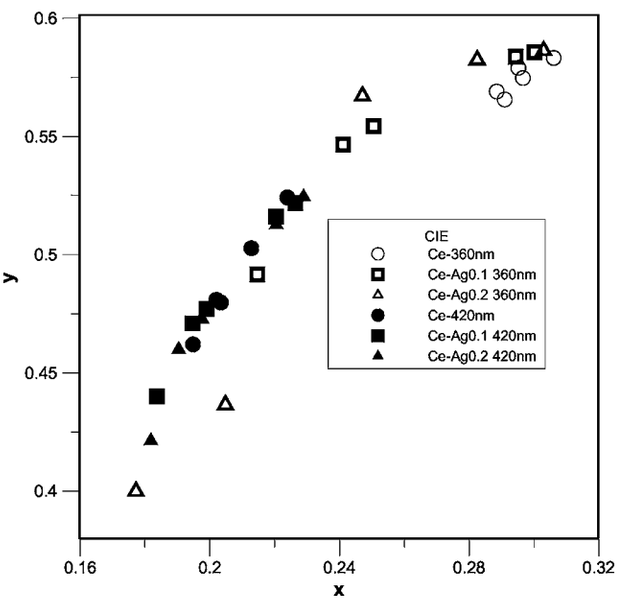

Figure 10. CIE color coordinate diagram of Ba_2ZnS_3:Ce^{3+}, Ag^+ phosphors.

mol % Ce^{3+} to exhibit yellowish-green luminescence and the PL intensity to peak at 498 nm with a CIE color coordinate of $x = 0.305$, $y = 0.524$.

Acknowledgments

The authors thank the National Science Council of the Republic of China for financially supporting this research under contract no. NSC-92-2216-E-006-009.

National Cheng Kung University assisted in meeting the publication costs of this article.

References

1. W. Lehmann, *J. Electrochem. Soc.*, **103**, 1389 (1970).
2. T. A. O'Brien, P. D. Rack, P. H. Holloway, and M. C. Zerner, *J. Lumin.*, **78**, 245 (1998).
3. F. Okamoto and K. Kato, *J. Electrochem. Soc.*, **130**, 432 (1983).
4. W. Lehmann and F. M. Ryan, *J. Electrochem. Soc.*, **118**, 477 (1971).
5. T. Morishita, H. Matsuyama, M. Matsui, S. Tonomura, and M. Wakihara, *Appl. Surf. Sci.*, **157**, 61 (2000).
6. D. Wauters, D. Poelman, R. L. Van Meirhaeghe, and F. Cardon, *J. Lumin.*, **91**, 1 (2000).
7. R. P. Rao, *J. Mater. Sci. Lett.*, **2**, 106 (1983).
8. S. Shionoya and W. M. Yen, *Phosphor Handbook*, pp. 177–200, CRC Press, Boca Raton, FL (1999).
9. P. Dorenbos, *J. Lumin.*, **91**, 91 (2000).
10. B. W. Arterton, J. W. Brightwell, B. Ray, and I. V. F. Viney, *J. Cryst. Growth*, **138**, 1051 (1994).
11. K. Kato and F. Okamoto, *Jpn. J. Appl. Phys., Part 1*, **22**, 76 (1983).
12. S. T. Lee, M. Kitagawa, K. Ichino, and H. Kobayashi, *Appl. Surf. Sci.*, **113-114**, 499 (1997).
13. R. Hoppe, *Angew. Chem.*, **71**, 457 (1959).
14. B. H. Megson, M.Sc. Thesis, Thames Polytechnic, London (1971).
15. S. Shionoya and W. M. Yen, *Phosphor Handbook*, pp. 217–230, CRC Press, Boca Raton, FL (1999).
16. G. Blasse, W. Schipper, and J. J. Hamelink, *Inorg. Chim. Acta*, **189**, 77 (1991).